

# POSITIVITY PROBLEM AND REACTIVE TRANSPORT SIMULATION IN POROUS MEDIA

ALAIN GENTY AND CHRISTOPHE LE POTIER

CEA Saclay, DANS/DM2S/SFME/MTMS, 91191 Gif-sur-Yvette Cedex, France.

## ABSTRACT

In the framework of high-level nuclear waste repository safety calculations, we developed the numerical platform Alliances allowing the coupling of several classical transport codes (MT3D, CAST3M) and geochemistry modules (PHREEQC, CHESS).

In order to avoid negative concentration calculation stemming from the transport model that may induce mass non-conservation, non consistent concentration field or geochemistry module failure, one generally uses for reactive transport simulations orthogonal meshes oriented along the main velocity direction. However, orthogonal meshes are not well adapted to describe field including cylindrical shapes (like wastes canisters, repository vaults, galleries) leading to coarse problem description or time consuming calculations.

In this paper, we investigate, on unstructured 2D mesh of cylindrical shape, the impact of using different spatial schemes (Mixed Hybrid Finite Elements, Finite Volumes) for the transport model including anisotropic heterogeneous dispersive tensor on negative concentration calculation and on reactive transport model in terms of concentration field and mass conservation errors.

## 1. INTRODUCTION

During the last decade, a large amount of work has been performed in the scope of reactive transport modelling in porous media leading today to a large number of geochemical transport codes [*Cheng and Yeh*, 1998, *Lucille et al.*, 2000, *Mugler et al.*, 2004, *van der Lee and De Windt*, 2001] based on the coupling of transport models and geochemistry modules.

To the authors knowledge, if those reactive transport codes are widely used for 1D problems, multidimensional applications are less used [*Molinero and Samper*, 2006]. In the latter case, one generally uses, for reactive transport simulations, orthogonal meshes oriented along the main velocity direction [*Cheng and Yeh*, 1998, *De Windt et al.*, 2003, *Mayer et al.*, 2001, *Prommer et al.*, 2002] in spite of the fact that orthogonal meshes are not always well adapted with regards to the studied problems. This is particularly the case in the context of high-level nuclear waste repository safety calculations where the description of the repository near field includes cylindrical shapes (like wastes canisters, repository vaults, galleries and drifts) and where the use of orthogonal meshes leads to coarse problem description and/or time consuming calculations.

The main motivation of using orthogonal meshes oriented along the main velocity direction is to avoid negative concentration calculation stemming from the transport model

that may induce mass non-conservation or non consistent concentration field in geochemistry module outputs as well as geochemistry module failure.

In this paper, we investigate on unstructured 2D mesh of cylindrical shape, the impact of using different spatial schemes, for the transport model including anisotropic heterogeneous dispersive tensor, on negative concentration calculation and on reactive transport model in terms of concentration field and mass conservation errors.

## 2. MATERIALS AND METHODS

**2.1. The Alliances Platform.** In the framework of high-level nuclear waste repository safety calculations, we developed a numerical platform allowing the coupling of several classical transport codes (MT3D [Zheng and Wang, 1999], CAST3M [Dabbène, 1998]) with geochemistry modules (PHREEQC [Parkhurst and Appelo, 1999], CHESS [van der Lee, 1998]) leading to a set of possible reactive transport codes. The coupling algorithm, written in a high level programming language (Python), is sequential iterative [Yeh and Tripathi, 1989].

**2.2. Test case.** We selected a scholastic case in order to test, the impact of using different spatial schemes for the transport on negative concentration calculation and on reactive transport model in terms of concentration field and mass conservation errors. This test problem is chosen in such a way that it can deal with diffusive advective anisotropic dispersive transport of contaminant through 2D cylindrical shape with a non parallel velocity field and presents an analytical solution.

It consists in leaching, on a disk of center  $O$  and radius  $r = R$ , an initial  $C = C_0$  concentration disk of center  $O$  and radius  $r = R_0$ , in a rotating velocity field  $\vec{V}$  of constant modulus  $\vec{V} = V_0 \vec{e}_\theta$ , with a fixed Dirichlet boundary condition  $C(r = R, t) = 0$ .

The determination of the radial analytical solution of the problem  $C(r, t)$  is described in details in the Appendix.

**2.3. Numerical schemes.** We intended to test four different spatial schemes for transport calculation: the Mixed Hybrid Finite Elements (MHFE) [Brezzi and Fortin, 1991, Dabbène, 1998], Finite Volumes (FV) (MPFA) [Aavatsmark et al., 1998, Le Potier, 2004], Finite Volumes (FV) (SYM) [Le Potier, 2005 a] and a new recently developed Finite Volumes (MON) scheme [Le Potier, 2005 b] that guaranties monotony and mass conservation.

**2.4. Meshes.** The calculations were performed on unstructured meshes of the domain made of triangular cells. In order to perform mesh convergence calculations four meshes of increasing refinement, presented in Figure 1, were used.

**2.5. Physical parameters.** The physical parameters values describing the rotating test case, namely, radius  $R$  (m) and  $R_0$  (m), velocity modulus  $V_0$  ( $m.s^{-1}$ ), porosity  $\omega$  (-), effective diffusion coefficient  $De$  ( $m^2.s^{-1}$ ), initial imposed concentration  $C_0$  ( $mol.m^{-2}$ ), longitudinal and transverse dispersivities  $\alpha_L$  (m) and  $\alpha_T$  (m), are presented in Table 1.

**2.6. Numerical parameters.** The calculations were conducted on each mesh described in Figure 1 using a constant time step  $dt = 5 \cdot 10^6 s$  ( $\simeq 60$  days) over a total period of  $10^{10} s$  ( $\simeq 300$  years).

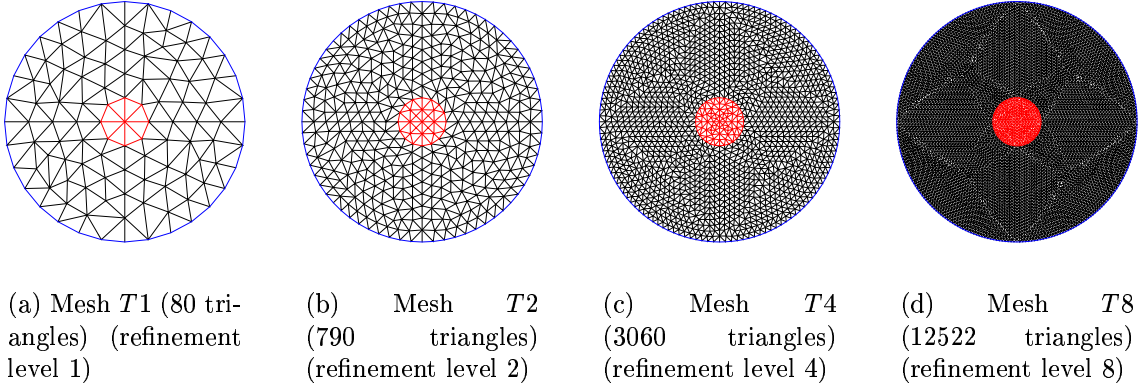


FIGURE 1. Unstructured meshes (triangles) of increasing refinement.

$R$ (m)	25	$R_0$ (m)	5	$V_0$ (m.s <sup>-1</sup> )	$1.10^{-10}$	$\omega$ (-)	1
$\alpha_L$ (m)	10	$\alpha_T$ (m)	1	$De$ (m <sup>2</sup> .s <sup>-1</sup> )	$1.10^{-10}$	$C_0$ (mol.m <sup>-2</sup> )	1

TABLE 1. Physical parameters values

### 3. RESULTS

In a first step we performed non reactive transport calculation using MHFE, FV (MPFA) and FV (MON) spatial schemes and in a second step we performed a reactive transport calculation. Results are analyzed in terms of maximum and minimum concentration values as well as mass conservation at different times.

**3.1. Non reactive transport calculations.** Results obtained with CAST3M transport code using MHFE, FV (MPFA) and FV (MON) spatial schemes are given in Table 2, 3 and 4, respectively.

Mesh	Time (s)	$C_{max}$ (mol.m <sup>-2</sup> )	$C_{min}$ (mol.m <sup>-2</sup> )	Mass error (-)
Mesh T1	$10^9$	0.96406	-0.02336	$-9 \cdot 10^{-8}$
	$10^{10}$	0.74677	-0.00462	$4 \cdot 10^{-7}$
Mesh T2	$10^9$	1.01456	-0.02742	$-2 \cdot 10^{-12}$
	$10^{10}$	0.93506	-0.00079	$-1 \cdot 10^{-11}$
Mesh T4	$10^9$	1.00748	-0.00740	$-3 \cdot 10^{-16}$
	$10^{10}$	0.95303	$-2 \cdot 10^{-7}$	$7 \cdot 10^{-16}$
Mesh T8	$10^9$	1.00007	$-5 \cdot 10^{-5}$	$-4 \cdot 10^{-15}$
	$10^{10}$	0.95511	$-1 \cdot 10^{-16}$	$-7 \cdot 10^{-15}$

TABLE 2. Results for transport calculation with CAST3M MHFE

Transport calculations performed using MHFE and FV (MPFA) methods exhibited negative concentration values especially for coarse mesh and early time calculation, while FV (MON) method guaranty the concentration monotony and mass conservation. It is to

Mesh	Time (s)	$C_{max}(mol.m^{-2})$	$C_{min}(mol.m^{-2})$	Mass error (-)
Mesh T1	$10^9$	0.98041	-0.01806	$-1 10^{-12}$
	$10^{10}$	0.79401	-0.00306	$9 10^{-9}$
Mesh T2	$10^9$	1.00546	-0.03070	$-2 10^{-16}$
	$10^{10}$	0.92721	-0.00077	$-7 10^{-14}$
Mesh T4	$10^9$	1.00194	-0.00317	$-7 10^{-16}$
	$10^{10}$	0.94943	$-1 10^{-6}$	$-2 10^{-15}$
Mesh T8	$10^9$	1.00007	$-6 10^{-5}$	$2 10^{-15}$
	$10^{10}$	0.95353	$-4 10^{-15}$	$-1 10^{-14}$

TABLE 3. Results for transport calculation with CAST3M VF (MPFA)

Mesh	Time (s)	$C_{max}(mol.m^{-2})$	$C_{min}(mol.m^{-2})$	Mass error (-)
Mesh T1	$10^9$	0.94028	$9 10^{-22}$	0.
	$10^{10}$	0.62454	$8 10^{-10}$	$3 10^{-9}$
Mesh T2	$10^9$	1.0442	0.	0.
	$10^{10}$	0.92453	$3 10^{-13}$	$1 10^{-12}$
Mesh T4	$10^9$	1.0429	0.	0.
	$10^{10}$	0.9701	$1 10^{-16}$	$7 10^{-16}$
Mesh T8	$10^9$	1.0111	0.	0.
	$10^{10}$	0.95816	$4 10^{-18}$	0.

TABLE 4. Results for transport calculation with CAST3M VF (MON)

note that, for this problem, negative concentration calculation occurred also for meshes constituted of squares (data not shown).

All the numerical spatial schemes were mass conservative (see Tables 2 3 and 4) and we checked, with the help of the analytical solution of the problem, the consistency of these schemes in  $L_2$  norm error on mesh of increasing refinement (data not shown). An example of the accuracy of the calculations can be seen on figure 2.

**3.2. Reactive transport calculations.** Reactive transport calculations were performed using a coupling of the transport calculation component CAST3M (using a MHFE spatial scheme) with the CHESS geochemical module. A set of chemical species as well as chemical reactions is needed by CHESS. In order to access the CHESS geochemical module without modifying our analytical solution of the problem, we defined a precipitation/dissolution reaction relating for a chemical species  $A$  its aqueous  $A_{aq}$  and precipitated  $A_{pr}$  parts with a solubility limit higher than the initial imposed  $A_{aq}$  concentration.

Calculations performed on highly refined mesh, where negative concentrations stemming from transport calculation are very small, were in good accordance with analytical solution, but for coarser mesh, the results of the reactive transport calculation were mass non conservative. The mass non conservation reached up to 3%. It is suggested that the geochemical module cut negative concentrations and then add some mass in the system. The same results were obtained using the transport calculation CAST3M code when we set to zero the negative concentration values after each calculation step.

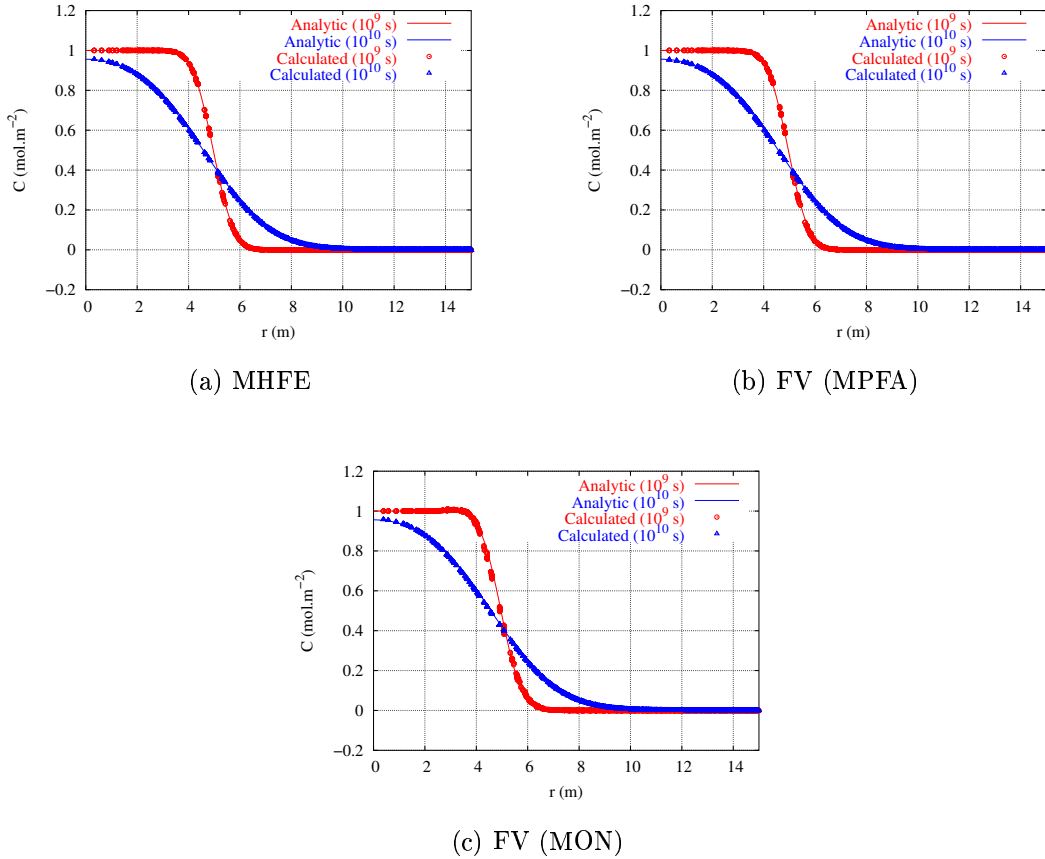


FIGURE 2. Comparison to analytical solution at time  $t = 10^9 s$  and  $t = 10^{10} s$  for mesh  $T8$ .

#### 4. CONCLUSIONS

We presented a test problem, dealing with diffusive advective anisotropic dispersive transport of contaminant on 2D cylindrical shape with a non parallel velocity field, leading, especially for coarse mesh and early time calculation, to negative concentration calculations with classical Mixed Hybrid Finite Element and Finite Volume methods.

We showed that the coupling of a transport code using those resolution methods with geochemical modules that cut negative concentrations conduct to reactive transport calculation tools that are mass non conservative (up to 3% in our case).

We also presented the transport calculation results obtained with a new Finite Volume method that guaranties the monotony of the calculated concentration and mass conservation. We checked on this test its accuracy. These results suggest to use the FV (MON) method for transport calculation in reactive transport tool in order to avoid mass non conservation and non consistency problems.

## 5. APPENDIX

**5.1. Analytical solution for the rotating test case.** The considered problem consists in leaching an initial concentration disk in a rotating velocity field with an external fixed Dirichlet boundary condition.

The mathematical description of this problem can be represented, in polar coordinates  $(r, \theta)$  based on  $(0, \vec{e}_r, \vec{e}_\theta)$ , by the way of transport equation (1) of nonreactive contaminant, including, advection, diffusion and kinematic dispersion processes [Marsily, 1986]

$$\omega \frac{\partial C}{\partial t} = \vec{\nabla} \cdot (\bar{D} \vec{\nabla} C - C \vec{V}) \quad (1)$$

subject to initial conditions

$$\begin{cases} C(r \leq R_0, \theta, t = 0) = C_0 \\ C(r > R_0, \theta, t = 0) = 0 \end{cases} \quad (2)$$

and boundary condition

$$C(r = R, \theta, t) = 0 \quad (3)$$

where  $\omega$  is the porosity,  $C(r, \theta, t)$  the solute concentration,  $t$  the time,  $\vec{V}(r, \theta, t) = V_0 \vec{e}_\theta$  the velocity and  $\bar{D}$  the diffusive-dispersive tensor expressed in  $(0, \vec{e}_r, \vec{e}_\theta)$  coordinates by

$$\bar{D} = \begin{pmatrix} D_e + \alpha_L V_0 & 0 \\ 0 & D_e + \alpha_T V_0 \end{pmatrix} \quad (4)$$

where  $D_e$  is the effective diffusion coefficient and  $\alpha_L$  and  $\alpha_T$  the longitudinal and transversal dispersivities respectively.

Due to the cylindrical symmetry of the problem ( $C(r, \theta, t) = C(r, t)$ ) and to the considered rotating velocity field of constant modulus ( $V(r, \theta, t) = V_0 \vec{e}_\theta$ ), the convective term  $\vec{\nabla} \cdot (C \vec{V})$  vanishes in equation (1) that reduces to

$$\omega \frac{\partial C}{\partial t} = \vec{\nabla} \cdot (\bar{D} \vec{\nabla} C). \quad (5)$$

Equation (5) can be developed in polar coordinates, from equation (4) defining  $\bar{D}$  and from the cylindrical symmetry of the problem implying that concentration  $C$  is only dependent on radius  $r$  and time  $t$ , to give

$$\frac{\partial C(r, t)}{\partial t} = D^* \left( \frac{\partial^2 C(r, t)}{\partial r^2} + \frac{1}{r} \frac{\partial C(r, t)}{\partial r} \right) \quad (6)$$

where  $D^* = \frac{D_e + \alpha_T V_0}{\omega}$  is a diffusive-dispersive coefficient.

Equation (6) is the classical radial diffusive equation for which a solution can be found by variable separation. Injecting  $C(r, t) = g(r) \cdot h(t)$  in equation (6) and considering that  $g$  and  $h$  are independent leads to the equation system (7) and (8)

$$\frac{\partial h(t)}{\partial t} + \alpha^2 D^* h(t) = 0 \quad (7)$$

$$\frac{\partial^2 g(r)}{\partial r^2} + \frac{1}{r} \frac{\partial g(r)}{\partial r} + \alpha^2 g(r) = 0 \quad (8)$$

where  $\alpha$  is a real positive.

The equation (7) presents a trivial solution  $h(t) = C_1 \exp(-\alpha^2 D^* t)$  where  $C_1$  is a constant. The equation (8) is the well known Bessel differential equation for which the solution writes  $g(r) = A_1 J_0(\alpha r) + B_1 Y_0(\alpha r)$  where  $A_1$  and  $B_1$  are constants, and  $J_0$  and  $Y_0$  are zero order Bessel function of the first and second species respectively. Notice that  $g(r)$  must be finite for  $r = 0$  implying that  $B_1 = 0$  because  $\lim_{r \rightarrow 0} Y_0(\alpha r) = +\infty$ .

The general solution of equation (6) is then obtained using a linear combination of the form

$$\boxed{C(r, t) = \sum_{k=0}^{\infty} E_k J_0(\alpha_k r) \exp(-\alpha_k^2 D^* t)} \quad (9)$$

where  $E_k$  and  $\alpha_k$  are calculated from initial and boundary conditions (2) and (3).

From boundary condition (3) we found that

$$C(r = R, t) = \sum_{k=0}^{\infty} E_k J_0(\alpha_k R) \exp(-\alpha_k^2 D^* t) = 0 \quad \forall t \quad (10)$$

implying that  $\alpha_k R$  are roots of  $J_0$

$$\boxed{J_0(\alpha_k R) = 0 \quad \forall k} \quad (11)$$

From initial condition (2) we found that

$$C(r, t = 0) = \sum_{j=0}^{\infty} E_j J_0(\alpha_j r). \quad (12)$$

Multiplying each side of equation (12) by  $r J_0(\alpha_k r)$ , integrating on  $r$  from 0 to  $+\infty$  and using commutativity of  $\sum$  and  $\int$  leads to relation (13).

$$\begin{aligned} \int_0^{+\infty} C(r, t = 0) J_0(\alpha_k r) r dr &= \int_0^{+\infty} \left( \sum_{j=0}^{\infty} E_j J_0(\alpha_j r) \right) J_0(\alpha_k r) r dr \\ &= \sum_{j=0}^{\infty} E_j \int_0^{+\infty} J_0(\alpha_j r) J_0(\alpha_k r) r dr \end{aligned} \quad (13)$$

Using orthogonality properties of Bessel function (14)

$$\int_0^{+\infty} J_0(\alpha_j r) J_0(\alpha_k r) r dr = 0 \quad \text{for } j \neq k, \quad (14)$$

then reducing the integration interval to  $[0, R]$ , allow to transform equation (13) into equation (15).

$$C_0 \int_0^{R_0} J_0(\alpha_k r) r dr = E_k \int_0^R J_0^2(\alpha_k r) r dr \quad (15)$$

Equation (15) allows then to calculate the  $E_k$  values using Bessel function properties (16) and (17) where  $J_1$  is the first order Bessel function of the first species,

$$\int_0^R J_0^2(\alpha_k r) r dr = \frac{R^2}{2} J_1^2(\alpha_k R) \quad \text{for } \alpha_k R \text{ root of } J_0 \quad (16)$$

$$\int_0^{R_0} J_0(\alpha_k r) r dr = \frac{R_0}{\alpha_k} J_1(\alpha_k R_0) \quad (17)$$

to obtain relation (18)

$$E_k = \frac{2C_0 R_0 J_1(\alpha_k R_0)}{\alpha_k R^2 J_1^2(\alpha_k R)} \quad (18)$$

Analytical solution of the problem is then defined by equations (9) (11) and (18).

#### REFERENCES

- Aavatsmark, I., T. Barkve, O. Boe and T. Mannseth (1998), Discretization on unstructured grids for inhomogeneous, anisotropic media, Part I: Derivation of the methods, *Siam J. Sci. Comput.*, *19*(5), 1700-1716.
- Brezzi, F. and M. Fortin (1991), *Mixed and Hybrid Finite Methods*, Springer-Verlag, New York.
- Cheng, H.-P. and G.-T. Yeh (1998), Development and demonstrative application of a 3-D numerical model of subsurface flow, heat transfer, and reactive chemical transport: 3DHYDROGEOCHEM, *J. Contam. Hydrol.*, *34*, 47-83.
- Dabbene, F. (1998), Mixed Hybrid Finite Elements for Transport of Pollutants by Undergrounds Water, Proc. of the 10<sup>th</sup> Int. Conf. on Finite Elements in Fluids, Tucson USA.
- De Windt, L., A. Burnol, P. Montarnal and J. van der Lee (2003), Intercomparison of reactive transport models applied to UO<sub>2</sub> oxidative dissolution and uranium migration, *J. Contam. Hydrol.*, *61*, 303-312.
- Le Potier, C. (2004), Finite volume in 2 or 3 dimensions for a diffusion convection equation applied to porous media with Cast3m, *2*, pp. 1015-1026, Proc. of the XV<sup>th</sup> Int. Conf. on Comput. Methods in Water Resources 2004, Elsevier.
- Le Potier, C. (2005), Finite volume scheme for highly anisotropic diffusion operators on unstructured meshes, *C.R. Acad. Sci.*, I *340*, 921-926
- Le Potier, C. (2005), Finite volume monotone scheme for highly anisotropic diffusion operators on unstructured triangular meshes, *C.R. Acad. Sci.*, I *341*, 787-792.
- Lucille, P.L., A. Burnol and P. Ollar (2000), CHEMTRAP: a hydrogeochemical model for reactive transport in porous media, *Hydrol. Proceed.* *14*, 2261-2277.
- de Marsily, G. (1986), *Quantitative Hydrogeology*, 440 pp., Academic Press, San Diego.
- Mayer, K.U., S.G. Benner, E.O. Frind, S.F. Thornton and D.N. Lerner (2001), Reactive transport modeling of processes controlling the distribution and natural attenuation of phenolic compounds in a deep sandstone aquifer, *J. Contam. Hydrol.*, *53*, 341-368.
- Molinerio, J. and J. Samper (2006), Large-scale modeling of reactive solute transport in fracture zones of granitic bedrocks, *J. Contam. Hydrol.*, *82*, 293-318.
- Mugler, Cl., A. Dimier and L. Trotignon (2004), Reactive transport modelling on the Alliances software platform. Proc. of the XV<sup>th</sup> Int. Conf. on Comput. Methods in Water Resources, Elsevier.
- Parkhurst, D.L. and C.A.J. Appelo (1999), User's guide to PHREEQC (version 2) - A computer program for speciation, batch-reaction, one-dimensional transport, and inverse geochemical calculations. Water-Resources Investigations Report 99-4259, U.S. Geol. Survey.
- Prommer, H., D.A. Barry and G.B. Davis (2002), Modelling of physical and reactive processes during biodegradation of a hydrocarbon plume under transient groundwater flow conditions, *J. Contam. Hydrol.*, *59*, 113-131.
- van der Lee, J. (1998), Thermodynamic and mathematical concepts of CHESS, Tech. Rep. LHM/RD/98/39, ENSMP (France).
- van der Lee, J. and L. De Windt (2001), Present state and future directions of modeling geochemistry in hydrogeological systems, *J. Contam. Hydrol.*, *47*, 265-282.
- Yeh, G.T. and V.S. Tripathi (1989), A critical evaluation of recent developments in hydrogeochemical transport models of reactive multichemical components, *Water Resour. Res.*, *25*, 93-108.
- Zheng, C. and P. P. Wang (1999), MT3DMS, A modular three-dimensional multi-species transport model for simulation of advection, dispersion and chemical reactions of contaminants in groundwater systems; documentation and user's guide, U.S. Army Engineer Research and Development Center Contract Report SERDP-99-1, Vicksburg, MS, 202 p.